# Near-resonant propagation of short pulses in a two-level medium

Xiang-yang Yu, Wei Liu, and Cheng Li

Phys. Rev. A **84**, 033811 — Published 9 September 2011

DOI: 10.1103/PhysRevA.84.033811

# Near-resonant propagation of short pulse in two-level medium

Xiang-yang YU*, Wei LIU and Cheng LI

*State Key Laboratory of Optoelectronic Materials and Technologies, Sun Yat-Sen University, Guangzhou 510275, China*
**Corresponding author: cesyxy@mail.sysu.edu.cn*

We present a numerical method for solving the Maxwell-Bloch equations describing pulse propagation for a two-level medium. The method is accurate, efficient, stable and well suited for this type of simultaneous equations. By applying the numerical scheme we investigate the evolutions of pulse area, pulse propagation, pulse velocity and spectral shapes under both homogeneous and inhomogeneous broadening conditions. The results show that, the area evolution and pulse reshaping procedure are significantly influenced by detuning and inhomogeneous line shape, which also impacts the oscillation tail and pulse-peak. Besides, the pulse-peak traces indicated the pulse velocity always increases with greater deviation in pulse area value from the value $2\pi$. We also demonstrate the pulse velocity increased for a larger detuning or a wider inhomogeneous line shape. Furthermore, spectral feature shows that pulse spectra evolve into an oscillating shape.

## I. INTRODUCTION

The coherent interaction of ultrashort optical pulses with resonant medium is a fundamental problem in quantum optics [1]. Recent advance in ultrafast laser technology has made it possible to generate extremely short and intense pulses such as single attosecond [2, 3] pulses. It has attracted much interest in the interaction of ultrashort pulse and atoms over the world. In the ultrafast regime, frequently in femtosecond, the relaxation has insufficient time to destroy the coherence, which makes the new phenomena of light-matter interaction becomes very interesting in such transient coherent processes.

In an inhomogeneously broadened medium, the famous area theorem [4] governs the coherent nonlinear transmission of ultrashort optical pulses through materials that have an absorption resonance frequency, which the atomic relaxation is neglected. Even the profile of few-cycle pulses evolution can still be predicted by the area theorem [5]. A new derivation of the area theorem including pulse chirping is also obtained and can be used to investigate pulse phase evolution [6]. In most theoretical analysis for pulses at the sub-femtosecond level, the effects of relaxation of the atomic system are neglected since the durations of the pulses are far smaller than the decay time. While considering the relaxation time, the effects of relaxation rate on pulse area evolution has been extensively investigated [7], which shows numerically that the stabilization of pulse area is not permanent because the energy losses that due to the spontaneous decay. By zero-area pulse [8], in the case of both off resonance and on resonance zero-area pulse can produce complete population transfer in a two state quantum system [9]. As to near-resonant case, it also presents the generalized pulse area is stabilized for relatively small detunings [10]. For the phase of ultrashort pulse in two-level systems, the measurement of pulse phase is studied in theory and experiment [11, 12]. As to the spectral behavior of a pulse passes through an atomic system, many literature is devoted to the spectral modifications [13], the spectral feature appears transition frequency and has significant deviation from a simple Lorentzian dip for larger pulse area [14,15]. The changes in the spectrum of a near-resonant pulse propagating through a two-level atomic system are also theoretically and experimentally studied [16]. It was shown that at the transition frequency the spectrum structure of the transmitted pulse depends sensitively on the pulse area, the pulse detuning and the absorption path length. Pulse shape is a visual display of pulse evolution in medium. It is reported that using a strong off-resonant ultrashort pulse one can control the shape of a weak, resonant, ultrashort pulse propagating in an assembly of two-level atoms [17]. Actually, without the driven pulse, the propagation of ultrashort laser pulses in a resonant atomic medium can leads to strong reshaping effects by dispersion [1, 18].

Despite the above extensive work, in comparison, only few theoretical or experimental studies [17] were devoted to the influence of the absorption spectral bandwidth on the pulse shape, the pulse velocity, the pulse spectrum and other pulse propagation properties. The inhomogeneous linewidth [1] of a medium characterizes the absorption spectral bandwidth. Big inhomogeneous linewidth means strong inhomogeneous broadening effect, and carrier frequency is included in absorption line. In the

opposite case, the absorption spectral bandwidth is very narrow and dominates closely around the central frequency (even can be represented by δ function). In this paper, we establish a powerful numerical scheme to simulate the light-matter interaction in two-level medium. By applying this accurate and effective numerical procedure, we analyze the evolution of pulse area to the case of nonzero detuning for different inhomogeneous linewidthes. To have further understanding the interaction of coherent pulses with medium, an extended study of the behaviors of pulse shape and velocity during propagation in a two-level medium was performed. With all these effects in mind we restrict our attention to the resonant and near-resonant interaction, and focus on the basic two-level system.

This paper is organized as follows. Sec. II the basic equations and definitions are introduced. Sec. III elaborates the numerical procedure and gives the flow chart. Sec. IV is devoted to a numerical analysis of the behaviors of the generalized pulse area and pulse propagation properties, and discusses the influence of pulse and medium parameters on the pulse velocity and spectral shapes. Finally, in Sec. V we present our conclusions.

## II. BASIC EQUATIONS AND DEFINITIONS

To study pulse propagation we solve the simultaneous Maxwell-Bloch equations for a two-level medium with the rotating-wave approximation, and consider the propagation in direction *z*. The Maxwell equation for propagation is

$$\dot{\Omega}_t(z,t)+cn^{-1}\cdot\dot{\Omega}_z(z,t)=\tau_0^{-2}\cdot\int_{-\infty}^{\infty}v\cdot g(\Delta)\mathrm{d}\Delta \quad (1)$$

where $\tau_0=(2\hbar n^2/N\mu_0c^2\mu^2\omega)^{1/2}$ is the effective time, $\Delta=\Delta_0+\omega-\omega_0$ is the detuning of the laser frequency $\omega$ from the resonance frequency $\omega_0$, and $\Delta_0$ is caused by inhomogeneous broadening. $g(\Delta)$ is the absorption line shape, such as line shape determined by Doppler broadening, $N$ is the atomic density, $n$ is the medium's refractive index, $\Omega(z,t)=\mu\tilde{E}(z,t)/\hbar$ is the Rabi frequency and $\tilde{E}(z,t)$ is the field envelope of the pulse, and $v(\Delta,z,t)$ is the component of the Bloch vector that determines the absorption of a single atom and can be calculated from the Bloch equations

$$\begin{aligned}\dot{u}_t&=-u/T_2-\Delta\cdot v\\ \dot{v}_t&=-v/T_2+\Delta\cdot u+\Omega\cdot w\\ \dot{w}_t&=-(w-w_0)/T_1-\Omega\cdot v\end{aligned} \quad (2)$$

here $w_0$ is the initial population difference between the upper and lower states and $T_1$ and $T_2$ are the longitudinal and transverse relaxation times, respectively. Dimensionless space and time variables by using $z'=nz/c\tau_0$, $t'=t/\tau_0$, $T_1'=T_1/\tau_0$, $T_2'=T_2/\tau_0$, $\Omega'=\Omega\tau_0$, $\Delta'=\Delta\tau_0$. For convenience, we record $z',t',T_1',T_2',\Omega'$, and $\Delta'$ as $z,t,T_1,T_2,\Omega$, and $\Delta$. Eqs. (2) are unchanged, but Eq. (1) is reduced to

$$\dot{\Omega}_t(z,t)+\dot{\Omega}_z(z,t)=\int_{-\infty}^{\infty}v\cdot g(\Delta)\mathrm{d}\Delta \quad (3a)$$

In Eq. (3a), the $g(\Delta)$ is the normalized inhomogeneous line shape. Before going further, we point out in homogeneously broadened medium, $g(\Delta)$ is too narrow to have effect on the integral term, and it was written

$$\dot{\Omega}_t(z,t)+\dot{\Omega}_z(z,t)=v(z,t) \quad (3b)$$

We define it as a Gaussian line shape function

$$g(\Delta)=\sqrt{2\ln 2/\pi\Delta_d^2}\cdot\mathrm{e}^{-\frac{2\ln 2}{\Delta_d^2}\Delta^2} \quad (4)$$

where $\Delta_d$ is the full width at half maximum of the inhomogeneous line shape (FWHM-ILS). The simultaneous solution of Eqs. (2) and Eq. (3) leads to fields that, when they are integrated over time at each propagation distance, give the area

$$S(z)=\int_{-\infty}^{\infty}\Omega(z,t')\mathrm{d}t' \quad (5)$$

which obeys the simple equation [2]

$$\frac{\mathrm{d}S}{\mathrm{d}z}=-\frac{\alpha}{2}\sin S \quad (6)$$

with $\alpha=\omega\pi\mu_0N\mu^2cg(0)/n\hbar$ is the linear optical attenuation coefficient for the material, and $g(0)$ is a Gaussian line shape with its maximum at $\Delta=0$. It proves useful to defined $\Omega$ as follows

$$\Omega(t)=\Omega_0\mathrm{e}^{-\frac{2\ln 2}{t_p^2}t^2} \quad (7)$$

where $t_p$ is the FWHM of Gaussian pulse and $\Omega_0$ is the pulse peak. Fourier transform solution of Eq. (7) shows the spectrum FWHM of input pulse is $\Delta_p=4\ln 2/t_p$.

## III. NUMERICAL PROCEDURE

Because, in general, the set of coupled Eqs. (2) and Eq. (3) cannot be solved analytically, numerical computations are necessary. In this section we describe the method of predictor-corrector fourth-order Runge-Kutta that we used to calculate the dynamical properties of Maxwell–Bloch equations. Our computational procedure includes the initial value predictor cycle and the corrector-predictor cycle. As we mentioned above, our method is designed to

simulate wave propagation through two-level medium. Since the emphasis here is on the numerical procedure, we show just the particular set of the coupled Eqs. (2) and Eq. (3).

In practice it is often useful for Eqs. (2), depend on time-differential only, to be solved by using the classical fourth-order Runge-Kutta scheme. This procedure is discussed in more detail in [15]. The method we use can be written as

$$\begin{aligned} u_{t+1} &= u_t + h_t(f_{u1} + 2f_{u2} + 2f_{u3} + f_{u4})/6 \\ v_{t+1} &= v_t + h_t(f_{v1} + 2f_{v2} + 2f_{v3} + f_{v4})/6 \\ w_{t+1} &= w_t + h_t(f_{w1} + 2f_{w2} + 2f_{w3} + f_{w4})/6 \end{aligned} \quad (8)$$

where $h_t$ is the step size for differentiation in time domain, $f_{ui}$, $f_{vi}$ and $f_{wi}$ are the right side of Eqs. (2), respectively. As illustrated in Fig. 1(a), the $m = T/h_t$, $T$ is the time length. Eq. (3) has important property that its characteristics depend on both space-differential and time-differential. We first consider the right-hand side of Eq. (3a). The integral term is a cumulative sum of inhomogeneous line shape (Fig. 1(b)), and can be rewritten in integral form as

$$\int_{-\infty}^{\infty} v(\Delta, z, t) \cdot g(\Delta) \mathrm{d}\Delta = \sum_k v(k\delta\Delta, z, t) \cdot g(k\delta\Delta)\delta\Delta \quad (9)$$

the $\delta\Delta$ is the step size of inhomogeneous line shape. For convenience, we record the right side of Eq. (9) as $\Sigma_{z,t}$ (in homogeneous broadened medium, Eq. (9) is neglected and $\Sigma_{z,t} = v(z,t)$ ). The simple finite-difference form of Eq. (3) is

$$(\Omega_{z+1,t+1} - \Omega_{z,t+1})/h_z + (\Omega_{z,t+1} - \Omega_{z,t})/h_t = \Sigma_{z,t+1} \quad (10)$$

where $h_z$ is the distance between any two space neighboring points. We assume the step size for differentiation in time is the same as the step size for differentiation in space for simplicity, which is $h = h_z = h_t$. Hence, it can be viewed as a rectangle in $z$ and $t$ space with a square mesh of points. Eq. (10) is reduced to

$$\Omega_{z+1,t+1} = \Omega_{z,t} + h \cdot \Sigma_{z,t+1} \quad (11)$$

In order to enhance the numerical calculation accuracy, we use the middle-grid-point to improve the simple finite-difference scheme. Thus

$$\Omega_{z+1,t+1} = \Omega_{z,t} + h \cdot (\Sigma_{z,t+1} + \Sigma_{z+1,t+1})/2 \quad (12)$$

In order to solve the coupled Eqs. (2) and Eq. (3), we apply a predictor-corrector scheme. To understand this technique, we first look at *the initial value predictor cycle*, the envelope function of the Rabi frequency is given by Eq. (7), in addition, we assume that the system initially contains no energy, which means $u_0 = 0$, $v_0 = 0$ and $w_0 = -1$ (all atoms at the ground state). We obtain $u$, $v$ and $w$ by applying the classical fourth-order Runge-Kutta scheme under determined value $\Delta$ and $z = 1$, then integrate the $u$ using Eq. (9) under determined value $z = 1$ when starting at $\Delta = -\infty$ and ending at $\Delta = \infty$, and finally substitute the $\Sigma_1$ into Eq. (11) to obtain next $\Omega$ ( $z = 2$ ) in time domain. As we show in Fig. 1(c).

During *the corrector-predictor cycle*, again using the fourth-order Runge-Kutta scheme and integrating the Eq. (9), and then substitute the $\Sigma_{z-1}$ and $\Sigma_z$ into Eq. (12) to obtain the corrected $\Omega_z$. We note that the corrected $\Omega_z$ should be used to correct the $u$, $v$ and $w$ under the value $z$. Again we substitute the obtained $u$ into Eq. (9) to get the integrating value $\Sigma_{z+1}$, and have the predictor value $\Omega_{z+1}$. As illustrated in Fig. 1(c), our program loop returns to the starting point of the corrector-predictor cycle under the condition of $z < l$ ( $l = L/h$, $L$ is the length).

We point out again that under the condition of in homogeneously broadened medium, the subroutine of the integral equations in the main routine flow chart shown in Fig. 1(c)., is neglected and replaced by the subroutine of partial differential Bloch equations. So *the initial value predictor cycle* and *the predictor-corrector cycle* no longer need to apply the integral procedure, other procedures are the same as described above.

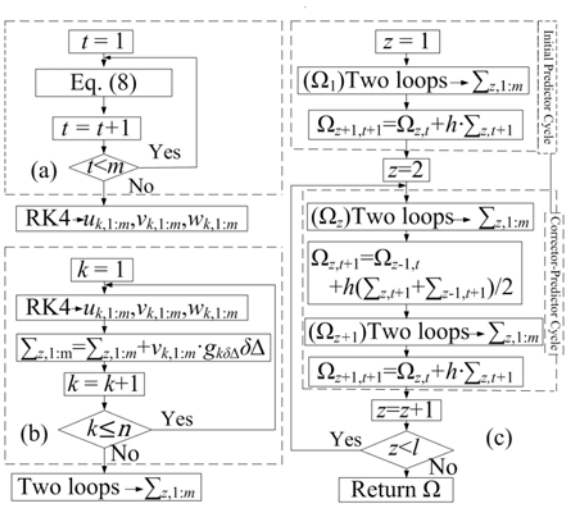


FIG. 1. Flow chart for subroutines of (a) Partial differential Bloch equations and (b) Integral equations, (c) Main routine flow chart.

The numerical procedure is now clear. In that way described above, we finally obtain the value of Ω describing the desired signal and the evolution of Bloch vector in both homogeneously and inhomogeneously broadened medium. Our method, compared with the finite difference method or general numerical scheme, has the advantage that it needs far

less calculation time (three or two orders of magnitude lower) for the same accuracy [20], which is discussed in the appendix.

## IV. RESULTS AND DISCUSSION

Now we apply the numerical procedure to investigate the behavior of the pulse propagation in a two-level medium. In the calculations relative units of time $\tau_0$ and distance $n/c\tau_0$ are used, and all other parameters are also given in relation to the scaled time $\tau_0$ (see in Sec. II).

### A. Pulse Area

Here we present a numerical analysis of the pulse area in homogeneously and inhomogeneously broadened two-level medium. We begin from the analysis of the behavior of the pulse area (according to Eq. (5), the definition pulse area is time integral starting at $-\infty$ and ending at $\infty$) during propagation. In The Area Theorem [1], it is obtained that the evolution of pulse area depends on the input pulse area and the linear optical attenuation coefficient for the material, and there are two striking consequences of the area theorem which are (i) pulse with special values of area, namely integer even multiples of π, will not change the pulse area but finally split into multiple 2π pulse; (ii) pulse area with other values is predicted to reshape into integer even multiples of π value, and also evolve into multiple 2π pulse [1,6]. Those properties can be shown to be stable in inhomogeneously broadened medium if the atomic relaxation is neglected.

The area theorem is not suitable for homogeneously broadened medium as presented in Fig. 2(a), in which we have plotted the area $S$ as a function of distance for different input area of the pulse. We restrict our calculations to the resonant and ultrashort pulses, and the time duration of the input pulse is neglected. It is obvious that the formed oscillation and its properties should strongly depend on the initial pulse area. To show this feature of the propagation we have analyzed the pulse behavior with different initial areas. The figure shows the pulse with $S(0)=1.3\pi$ needs very short distance (almost $z=0.02$ ) to approach 2π and then oscillates around the value 2π. The continuous oscillation amplitude becomes smaller as raising distance; and the oscillation period, is a function of the distance, becomes longer with the increasing of distance. As compared with the pulses having areas of 1.5π and 1.9π, the pulse with larger area needs shorter distance to approach 2π, and the oscillation period and amplitude are also decreased relatively. While the initial input pulse area is 2π, the pulse area remains unchanged and with no oscillation, actually, the shape and peak amplitude of the pulse are stable as it propagates through the medium.

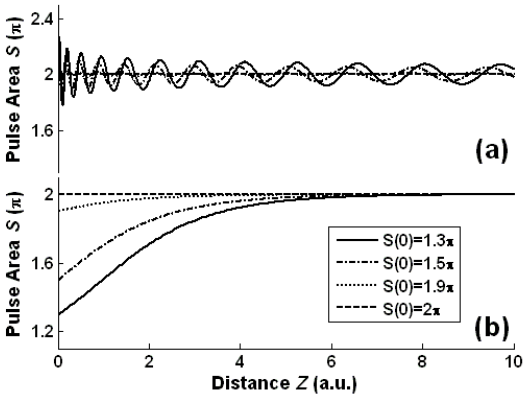


FIG. 2. The spatial evolution of pulse area for four values of input pulse area in (a) Homogeneously and (b) Inhomogeneously broadened medium.

The presence of our numerical calculations in Fig. 2(b) shows that the smaller the initial pulse area is, the longer the optical path needed to approach 2π. Exactly, it proves that the area evolution in inhomogeneously broadened medium strictly obey the area theorem in the absence of relaxation time.

One of the most interesting results of the area evolution in a medium is the effect of the inhomogeneous line shape. Here we give a few results showing the influence of the FWHM-ILS $\Delta_d$ which characterizes the inhomogeneous line shapes $g(\Delta)$ on this effect. Fig. 3 shows the process of a pulse in resonance and with an input area $S(0)=1.5\pi$ converts into a 2π pulse. In general, for relatively large value of $\Delta_d$ (= 3), the evolution curve of pulse area to approach 2π is smooth. As to the value of $\Delta_d=0.3$, the distance of the 1.5π pulse approaching to 2π is relatively shortened, and there comes out an oscillation tail. The decrease of $\Delta_d$ (such as the dot curve) results in the shortening of the approaching distance, and makes the oscillation increasingly stronger. Compared with the area evolution in Fig. 2(a), we find out that the smaller value of $\Delta_d$ is, the closer the evolution properties are. Actually, homogeneous broadening is the limit of $\Delta_d$ tends to zero [1].

In previous discussions of area evolution, we ignored both longitudinal and transverse relaxation effects. In general, the longitudinal relaxation time $T_1$ is far greater than the transverse relaxation time $T_2$, so the parameter used correspond to the calculation can be chosen as $T_1=10T_2$. Fig. 4(a) shows the area evolution of the pulse with $S(0)=1.7\pi$ as a function of propagation distance for different $T_2$ in

homogeneously broadened medium. The general picture for each case is similar. For longer propagation distance, the pulse area no longer oscillates around the value 2π and almost stiff decreases to the 0π value. Since the lacking of energy by increasing value of $T_2$, the pulse is not able to stabilize and makes itself transform into 0π pulse. The analysis of Fig. 4(a) indicates that the larger $T_2$ is, the longer distance it can propagate. As to inhomogeneously broadened medium (see Fig. 4 (b)), the evolution form of pulse area also transform into 0π pulse due to the relaxation and energy losses, and the area of the pulse with $T_2 = 10$ does not even reach the 2π value. It is obvious that the collapse curves, from 2π to 0π, are much smoother than the curves under homogeneous broadening condition. This effect can be explained by the pulse energy losing procedure [7].

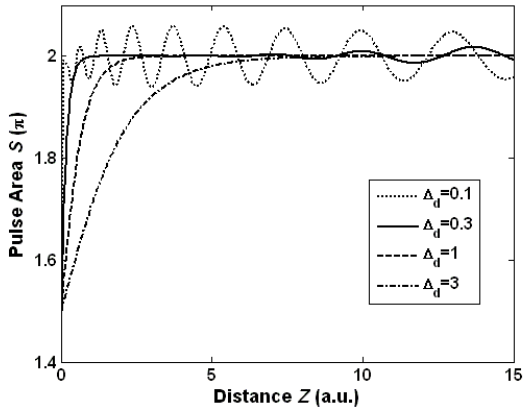


FIG. 3. Evolution of pulse area as a function of propagation distance for different FWHM-ILS.

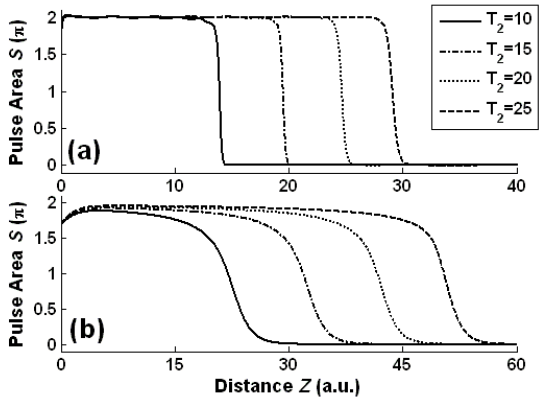


FIG. 4. The spatial evolution of pulse area for different relaxation times in (a) Homogeneously and (b) Inhomogeneously broadened medium.

The interesting evolution behavior of pulse area in Fig. 5(a) shows the influence of detuning in homogeneously broadened medium. In the near-resonant case with $\Delta = 0.1$, the propagation distance before the pulse area approaching to 2π is obviously increased. As the detuning Δ shifts toward bigger, a longer propagation distance under the area value of 1.7π is observed. That means the detuning delays the converting procedure and makes the input pulse more stable at its initial area value, i.e., $\Delta = 0.3$, the pulse oscillates around the value 1.7π for a propagation length almost 40. However, under inhomogeneous broadening condition, the area evolution of resonant pulse propagation with detuning still mainly obeys the area theorem (see Fig. 5(b)), and the impact is much smaller compared with Fig. 5(a).

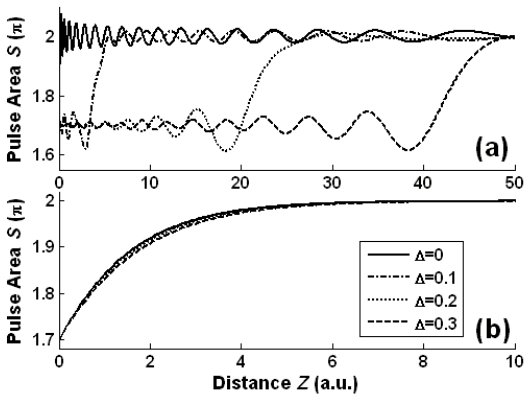


FIG. 5. Pulse area as a function of distance for different detuning values in (a) Homogeneously and (b) Inhomogeneously broadened medium.

We therefore conclude that in atomic media with decay mechanism, whether the medium is inhomogeneous or homogeneous broadening, the pulse with whatever area value will collapse into 0π. Moreover, in the present paper of homogeneous broadening condition, the detuning plays an important role in the evolution of pulse area, but has relatively slight influence on the behavior of area evolution in inhomogeneously broadened medium.

### B. Pulse Shape

We now turn to investigate the pulse propagation. The results of the propagation of a 1.7π pulse in homogeneously broadened medium are presented in Fig. 6. It can be seen that the pulse propagation process is interesting, the pulse shape is obviously deformed and there exists an oscillation tail beside the main pulse, and the peaks of the Rabi-frequency are not stable. Combining with the area evolution in Fig. 2(a), we believe that the unstable peaks make the area necessarily oscillate around the value 2π.

Furthermore, we also study the propagation behavior of pulses with other area values, e.g., 1.5π pulse, 1.9π pulse and 2π pulse. All compared pulses propagate under the same condition. We find that during the reshaping procedure, the closer the initial pulse area to 2π the more stable the Rabi-frequency performed (with neglective oscillation tail and more stable peaks).

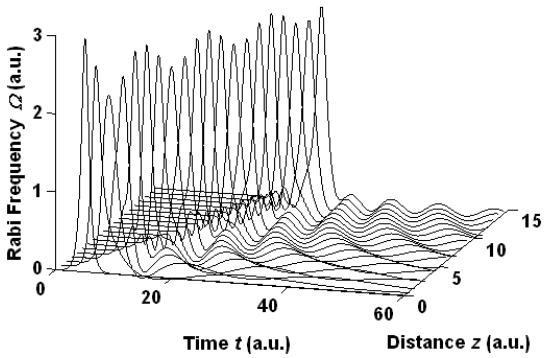


FIG. 6. Evolution of a 1.7π pulse in homogeneously broadened medium, $\Delta = 0$.

While considering the influence of detuning (again) on the pulse propagation, we plot the peaks curve of Rabi-frequency in Fig. 7. The solid curve, without detuning, presents a stiff decrease after propagating in the medium for a short distance, and evolves into an oscillating structure. As to $\Delta = 1$, we observe the oscillations of peaks curve diminished. For the bigger detunings (plotted in dashed and dashed-dot curves), the peak value slowly and smoothly decays. Accurately, if we plot the pulse evolution with different detunings in a three-dimensional space-time, we'll find big detuning slows down the pulse reshaping process and inhibits the oscillation. Actually, because the spectrum width interaction with atoms in homogeneously broadened medium is very narrow, a small detuning will hinder the interaction to some extent.

As in the inhomogeneously broadened medium, the pulse behaves in a similar way with the performance in Fig. 6, see Fig. 8(a) under slightly FWHM-ILS, where we neglect the relaxation and detuning. For the bigger detuning plotted in Fig. 8(b), the results suggest that both of the main pulse and oscillation tail transform relatively stable for FWHM-ILS $\Delta_d = 1$. Obviously, increasing the FWHM-ILS further such that the pulse peak reshaping can be obtained in a smooth and slow decrease process, and the oscillating structure almost disappeared. Theoretically, for the same incident pulse, the pulse spectrum is fixed, only the atoms with resonant frequency can have interaction with the pulse. Increasing FWHM-ILS means that the rate of active atoms near the central resonant frequency diminishes. That is the reason why big $\Delta_d$ slows the area evolution shown in Fig. 3.

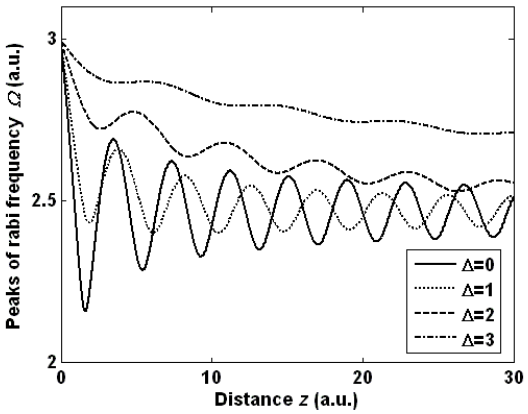


FIG. 7. Evolution of 1.7π pulse for different detunings in homogeneously broadened medium.

As we know, pulse breakup occurs when the pulses with areas above 3π due to the stimulated absorption and reemission processes [1, 21]. The pulse breakup depends on various parameters, including the pulse area, the atomic density and so on. In Fig. 9 we compare the propagation properties of pulses for different $\Delta_d$. We see that after a small optical path the pulses breakup are observed, the first part sharpens and the second part widens during propagation. The evolution of the first part is the same as Fig. 8 shown, and the second part, whose area is also converted to 2π but with slower velocity and lower energy. When the $\Delta_d$ is so small that the pulse breakup in the medium occurs more easily (in Fig. 9(a)) with relatively short optical path, as to increasing $\Delta_d$, only for a longer optical path will the pulse encounter a sufficient number of atoms to cause reshaping. After the pulse propagates further through the medium, we can find the velocity of the second parts are obviously different in the three figures.

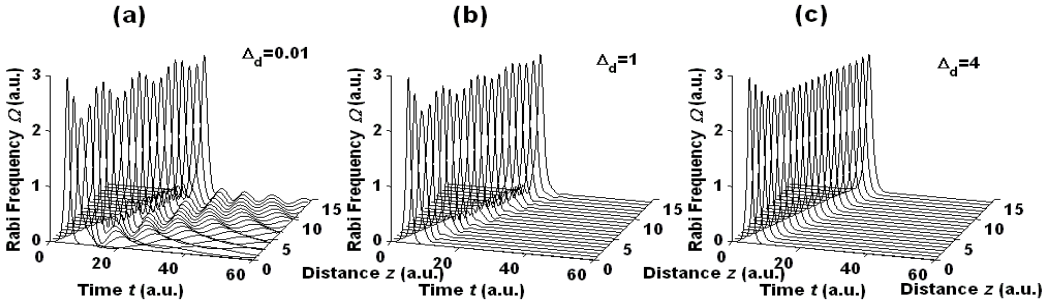


FIG. 8. Evolution of 1.7π pulse for different FWHM-ILS.

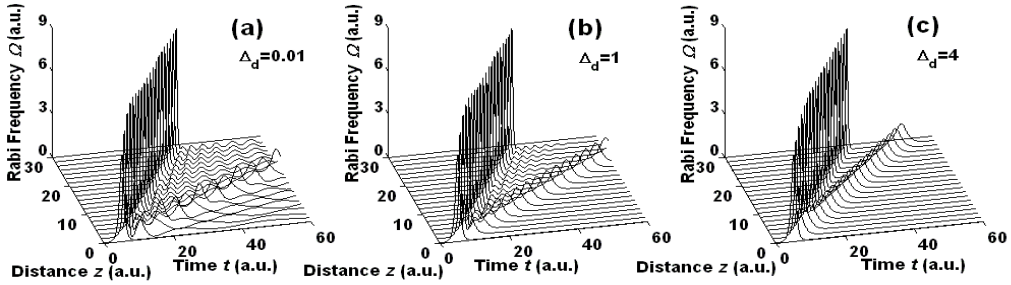


FIG. 9. Evolution of 3.4π pulse for different FWHM-ILS.

Coming to the end of our discussion of the ultrashort pulse propagation, we want to emphasize the propagation relationship between the homogeneous and inhomogeneous broadening. In general, for quite big $\Delta_d$ only the central part of the spectrum is active and the pulse shapes, including both the pulse peaks and with strong or weak oscillation tail, are also depended mainly on it.

### C. Pulse Velocity

Another important feature of pulse propagation in medium is the velocity, which is influenced not only by the pulse properties but also by the optical materials. For ultrashort pulse, we use the main pulse peaks to mark pulse trace, and pulse velocity is reflected according the corresponding space-time coordinates of the curves.

In the previous sections, we have shown that pulses have reshaping procedure during their propagation in absorbing medium, and pulse initial areas have significant influence on the evolutions of pulse area. Fig. 10 presents the peaks evolution that reflects the velocity of the pulse. As the optical path is a constant, we find that the pulse with initial area $S(0)=1.6\pi$ needs the maximum time among the four curves, and pulse with initial area $S(0)=1.7\pi$ needs relatively short propagation time. With the increasing of pulse area (<2π), the needed time becomes shorter and shorter, which means the propagation velocity is increased. A close look at the four curves structure shows the following feature: At exactly the early evolution, the trace of solid curve is not stable and the velocity of pulse peak dramatically oscillates. Gradually, solid curve deviates from the initial direction, and pulse peak velocity becomes to be flat, within 0.5*c*-0.8*c* [22]. Actually, whatever the medium is homogeneous or inhomogeneous broadening, the reshaped pulse broadens its width, losses its energy and slows down.

We also present the numerical study of detuning effect on the pulse velocity. If compare the four curves we can say roughly that for pulse without detuning $\Delta=0$ the propagation time is the maximum, and for the pulse having detuning $\Delta=1$ it observes the needed propagation time is shortened. With the further increasing of detuning, the propagation time is pulled toward a limited value. In general, an increase of detuning means the rate of active atoms is diminished, which results in weakened the interaction between the pulse and medium. Meanwhile, the pulse velocity is naturally increased in the medium but will not exceed the speed of a pulse with initial area value 2π.

In this present section, we have shown numerically that the pulse velocity in medium is always increased with the greater deviation in pulse area value from the value 2π, and also observe an increase in detuning or FWHM-ILS can cause the pulse velocity to increase. The physical mechanisms are given theoretically.

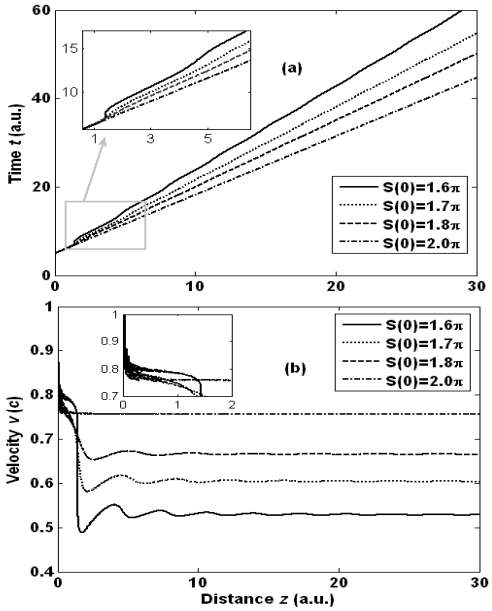


FIG. 10. Evolution of pulse peaks for different input pulse areas in homogeneously broadened medium. (a) In dimensionless time. (b) In term of light velocity *c*.

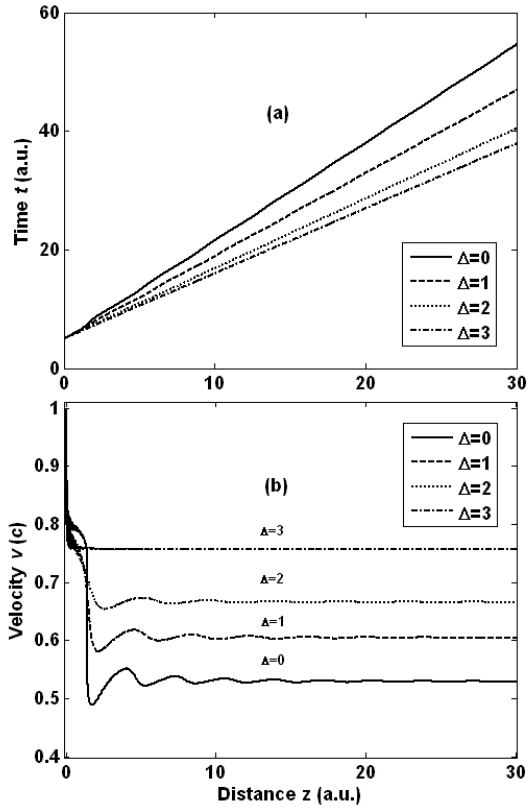


FIG. 11. Evolution of 1.7π-pulse peaks for different detuning in homogeneous broadened medium. (a) In dimensionless time. (b) In term of light velocity *c*.

In Sec. IV part A, we studied the influence of $\Delta_d$ on area evolution and given the important results. Furthermore, we investigate the influence of $\Delta_d$ on the pulse velocity in our model. Fig. 12(a) presents the behavior of pulse peaks with initial area 1.5π for various $\Delta_d$. Expectedly, an increasing in the $\Delta_d$, the pulse velocity becomes more greater because the rate of active atoms near the central resonant frequency diminishes, this statement has confirmed by the results presented in Fig.3 and Fig. 8. We also illustrate the evolution of pulse with initial area value 1.8π for the same $\Delta_d$. Fig. 12(b) shows the evolution curves shifts toward the direction of smaller time, and the distance between the adjacent curves is also compressed. While the initial area is 2π, trends mentioned above will be further enhanced. On the other hand, the influence of $\Delta_d$ becomes weaker.

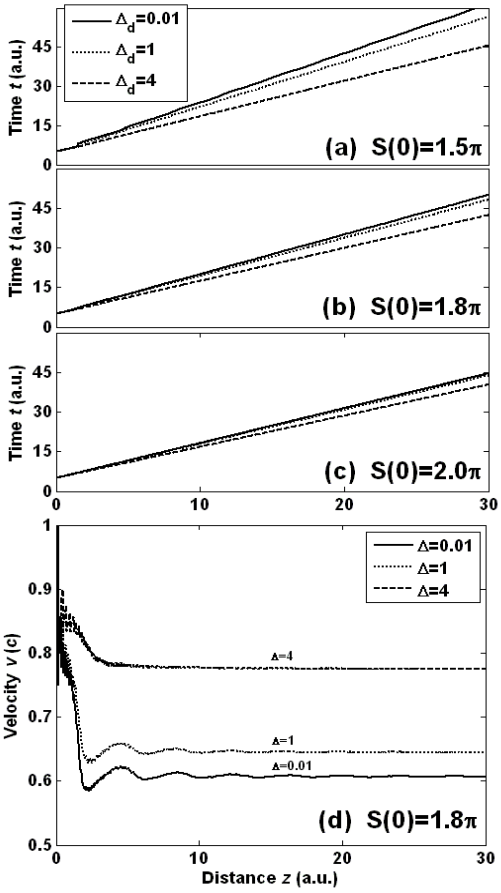


FIG. 12. Evolution of pulse peaks for different FWHM-ILS in inhomogeneously broadened medium. (a), (b) and (d) In dimensionless time. (d) In term of light velocity *c*.

### D. Pulse Spectrum

In this section we discuss the influence of pulse area, detuning, and distance on the spectrum of input pulse. In the case of inhomogeneous broadened medium, the spectral shapes are similar with homogeneous broadened medium, by averaging atomic variables over a Doppler profile width [16].

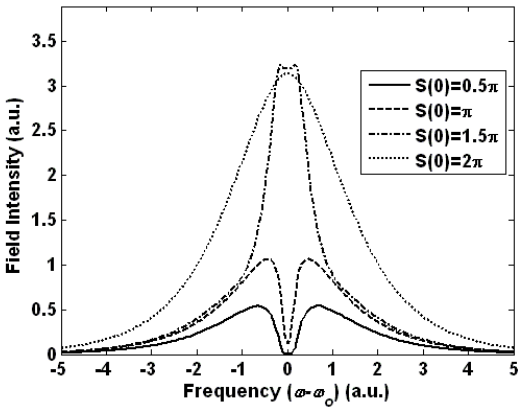


FIG. 13. Spectral shapes of pulse at z=1 for different pulse area in homogeneous medium.

In Fig. 13, we plot the spectrum of different pulse area, propagating in homogeneous broadened medium with $T_1$=10, $T_1$=10$T_2$ and Δ=0. From the discussion of Fig. 4, we choose the small distance of $z$ ($z$ = 1) and in this situation pulse area does not decrease sharply. Frequencies near the atomic frequency show a dip on account of the interaction of dipole field and the pulse.

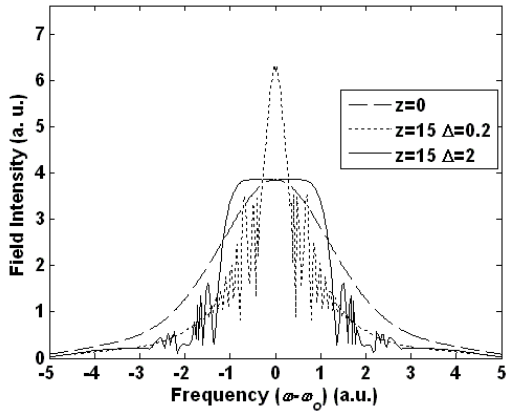


FIG. 14. Spectral shapes of 1.25π-pulse for different detuning in homogeneous broadened medium: longitudinal time $T_1$ and transverse time $T_2$ are both ignored.

When detuning is taken into consideration in Fig. 14, spectral shapes of the pulse evolve into oscillating structure especially around resonant frequency. Meanwhile frequencies near atomic frequency are amplified.This effect is related to the procedure of light reemission [10, 23].

## V. CONCLUSIONS

In conclusion, we have presented a predictor-corrector fourth-order Runge-Kutta method for integration of the Maxwell-Bloch equations with partial differential and integral terms. Since the characteristics are used, the Bloch equations only contain a partial derivative with respect to time independent variable, thus permitting us to apply the fourth-order Runge-Kutta method; the Maxwell equation, we choose a middle-grid-point scheme to enhance the calculation accuracy; as to the predictor-corrector method, which effectively improves the accurate results and greatly saves calculation time.

Then, applying the numerical method we study the evolutions of pulse area, pulse propagation and pulse velocity under both homogeneous and inhomogeneous broadening conditions. We prove again that pulse area will collapse into zero under the decay mechanism, and find the FWHM-ILS and detuning have significantly influence on area evolution. The influence under homogeneous broadening condition is more obvious than in inhomogeneously broadened medium. As to pulse reshaping procedure, we point out that the oscillations of pulse-peak curve and tail mainly determined by the value of FWHM-ILS, and also effected by detuning. Additionally, we discuss pulse breakup under various FWHM-ILS and find pulse velocity changed obviously. Besides, we give the pulse peak trace that presents the pulse velocity to some extent. For various initial input pulse areas, it shows the pulse velocity becomes greater as the pulse area getting closer to 2π, and a bigger detuning also creates greater pulse velocity. As to inhomogeneously broadened medium for the same medium, bigger FWHM-ILS causes the pulse velocity in the medium relatively greater. Finally, we discuss the evolution of the pulse spectrum in homogeneous medium. The spectral shapes demonstrate that with absorption the frequencies near atomic frequency are absorbed. In the case of without consideration of absorption, spectral shapes show an oscillating and complex structure.

## ACKNOWLEDGMENTS

This work is supported by the National Natural Science Foundation of China under Grant No.10574166 and the Guangdong Natural Science Foundation under Grant NO. 8151027501000062

## APPENDIX

We get some other methods in comparison with predictor-corrector fourth-order Runge-Kutta. The part of Bloch equation adopts Eq. (8), but the part of Maxwell uses different metholds.

Method I: Predictor-corrector fourth-order Runge -Kutta:

$$\Omega_{z+1,t+1} = \Omega_{z,t} + h \cdot (v_{z,t+1} + v_{z+1,t+1})/2 . \quad \text{(A1)}$$

Method □: Square mesh of points (discussion of Eq. (11) in Sec. Ⅲ),

$$\Omega_{z+1,t+1} = \Omega_{z,t} + h \cdot v_{z,t+1} . \quad \text{(A2)}$$

Method □ : Backward difference method,

$$\Omega_{z+1,t+1} = \Omega_{z,t} + h \cdot v_{z,t} . \quad \text{(A3)}$$

We compare numerical solution by different methods with annalytical solution by hyperbolic-secant pulse at $z = 4$ (units of $c\tau_0 / n$), pulse area $S(0)=2\pi$, detuning $\Delta = 0$, and pulse duration $t_p = 1$ (units of $\tau_0$).

TABLE. Ⅰ. Step effects on the maximum global error of method Ⅰ, Ⅱ, Ⅲ, respectively.

| Step $h$ | Analytic Solution Ⅰ | Method Ⅰ | Error Ⅰ | Analytic Solution Ⅱ | Method Ⅱ | Error Ⅱ | Analytic Solution Ⅲ | Method Ⅲ | Error Ⅲ |
|---|---|---|---|---|---|---|---|---|---|
| 0.01 | 2.4847502 | 2.5244935 | 0.0397433 | 2.2538526 | 3.2770607 | 1.0231534 | 2.8965887 | 2.3250312 | 0.5715574 |
| 0.005 | 2.5010517 | 2.4808136 | 0.0202381 | 2.4855154 | 3.0013508 | 0.5158354 | 2.7929807 | 2.5021345 | 0.2908462 |
| 0.001 | 2.4730871 | 2.4689348 | 0.0041523 | 2.6620791 | 2.7651681 | 0.1030890 | 2.7019673 | 2.6430887 | 0.0588786 |

It can be seen from the Table Ⅰ, in the case of same step, the error of method Ⅰ are smaller 1 or 2 orders of magnitude than errors of menthod Ⅱ and method Ⅲ. From the longitudinal view, the step is havled, and errors are half, which means method Ⅱ and method Ⅲ, in order to get the same accuracy as method □, must adopt smaller step and spend more time.

In order to verify the convergence and reliability of the method, we compare the analytical solution of the evolotion of pulse area in inhomogeneous medium with numerical solution. We adopt hyperbolic-secant pulse and laser parameters are as follows: the longitudinal and transverse relaxation time $T_1$=0, $T_2$=0, detuning $\Delta$=0, and step $h$=0.02. In Table Ⅱ we get the influence of the propagation distance on the abosolute errors of pulse areas, and results show that with the increase of propagation distance the absolute errors between numerical solution and analytical solution get smaller. Besides, the maximum global errors of 2π pulse also get smaller as the increase of distance [20]. As is mentioned above, it shows the convergence and reliability of the method.

TABLE. Ⅱ. Comparison of pulse area evolution for numerical solution and analytic solution. The initial input pulse areas are 1.3π, 1.5π, 1.9π and 2π respectively.

| | Pulse area | $z$=3 | $z$=6 | $z$=9 | $z$=12 | $z$=15 |
|---|---|---|---|---|---|---|
| Absolute errors | 1.3π | 0.0035 | 0.0012 | 9.0198e-5 | 6.5447e-6 | 1.7721e-6 |
| | 1.5π | 0.0043 | 6.2639e-4 | 4.5997e-5 | 3.3658e-6 | 2.5447e-7 |
| | 1.9π | 0.0012 | 8.9803e-5 | 6.6600e-6 | 5.7334e-7 | 1.2950e-7 |
| Maximum global errors | 2.0π | 0.0291 | 0.0290 | 0.0288 | 0.0287 | 0.0278 |

1. L. Allen and J. H. Eberly, *Optical Resonance and Two-Level Atoms* (Wiley, New York, 1975).
2. T. Brabec and F. Krausz, Rev. Mod. Phys. **72**, 545–591 (2000).
3. M. Hentschel, R. Kienberger, Ch. Spielmann, G. A. Reider, N. Milosevic, T. Brabec, P. Corkum, U. Heinzmann, M. Drescher and F. Krausz, Nature **414**, 509–513 (2001).
4. S. L. McCall and E. L. Hahn, Phys. Rev. Lett. **18**, 908–911 (1967).
5. Jian Xiao, Zhongyang Wang and Zhizhan Xu, Phys. Rev. A **65**, 031402 (2002).
6. J. E. Eberly, Opt. Exp. **2**, 173-176 (1998).
7. A. I. Maimistov, J. Fiutak and W. Miklaszewski, Z. Phys. B **88**, 349–358 (1992).
8. Joshua E. Rothenberg, D Grischkowsky, and A. C.Balant. Phys.Rev. Lett **53**. 552-555 (1984).
9. G. S. Vasilev and N. V. Vitanov. Phys. Rev. A **73**, 023416 (2006).
10. W. Miklaszewski, J. Opt. Soc. Am. B **12**, 1909-1917 (1995).
11. Joshua E. Rothenberg and D. Grischkowsky. J. Opt. Soc. Am. B **3**, 626-633 (1985).
12. Joshua E. Rothenberg and D. Grischkowsky. J. Opt. Soc. Am. B **2**, 1235-1238 (1986).
13. A. Lipsich, S. Barreiro, A. M. Akulshin and A. Lezama, Phys. Rev. A **61**, 053803 (2000) and references therein.
14. J. C. Diels and E. L. Hahn, Phys. Rev. A **8**, 1084–1110 (1973).
15. N. Schupper, H. Friedmann, M. Matusovsky, M. Rosenbluh and A. D. Wilson-Gordon, J. Opt. Soc. Am. B **16**, 1127-1134 (1999).
16. Jinendra K. Ranka, Robert W. Schirmer and Alexander L. Gaeta, Phys. Rev. A **57**, R36–R39 (1998).
17. J. C. Delagnes, F. A. Hashmi and M. A. Bouchene, Phys. Rev. A **74**, 053822 (2006).
18. J. C. Delagnes and M. A. Bouchene, Phys. Rev. A **76**, 023422 (2007).
19. John H. Mathews and Kurtis D. Fink, *Numerical Methods Using MATLAB* (Publishing House of Electronics Industry, Beijing, 2005).
20. LI Cheng, ZHANG Huarong and YU Xiangyang, Acta Scientiarum Naturalium Universitatis Sunyatseni **48**, 36–41 (2009).
21. W. Miklaszewski and J. Fiutak, Z. Phys. B **93**, 491–499 (1994).
22. D. Grischkowsky, Eric Courtens, and J. A. Armstrong. Phys. Rev. Lett **31**, 422-425.
23. J. C. Delagnes and M. A. Bouchene. 76. Phys. Rev. A **76**, 023422(2007).